Supporting Information

Imai et al. 10.1073/pnas.1108372108

SI Materials and Methods

Antibodies and Reagents. Mouse anti-HSP90α mAb (EMD-17D7) was from Calbiochem. Rat anti-HSC70 (1B5) and mouse anti-KDEL mAbs were obtained from StressGen Biotechnology. Rabbit anti–HSP90β-specific antibody was from Lab Vision Corporation. Mouse anti-19S Rpt1 mAb was from Biomol International. Rabbit anti-sec61β was from ABR. Fluorochrome-conjugated antibodies against CD4, CD8, CD11c, CD86, I-A^b, and H-$2K^b$ were purchased from BD Pharmingen. Mouse anti-HSP90 mAbs (2A6-E9, 4B6-G12) and mouse anti-OVA serum were generated in our laboratory. Anti-CD8α and -CD11b magnetic particles were from BD Bioscience. Alexa Fluor 647 (AF647), FITC protein labeling kit, and Dynabeads M-280 sheep antimouse IgG were from Invitrogen. CNBr-activated sepharose was from GE Healthcare. The protein biotinylation kit, Ezlink sulfo-NHS-LC-LC-biotin, was from Thermo Scientific. OVA and BSA were from Sigma, and OVA was used as a model antigen. Japanese cedar pollen allergen Cryj1, purified (Cryj), was from Hayasibara Biochemical Laboratories. The surface HSP90 inhibitor geldanamycin–FITC (GA–FITC) and the proteasome inhibitor epoxomicin were from Biomol. The subcellular proteome extraction kit was from Calbiochem. All other reagents were purchased from Sigma.

Generation of HSP90α-Null Mice. A genomic clone containing the *Hsp90aa1* gene was obtained from BACPAC library of C57BL/6 genomic DNA (Children's Hospital Oakland Research Institute). The region from exon 9 to exon 11 of the *Hsp90aa1* gene was subcloned into pBluescript II SK(−) vector (Stratagene) and a loxP was inserted between exon 10 and exon 11. The fragment from exon 9 to exon 11 containing loxP was subcloned into pLNTK vector (1) downstream of a 3′ loxP-flanked Neo cassette. To generate the targeting vector, the region from exon 4 to exon 8 of the *Hsp90aa1* gene was subcloned into the pLNTK vector between the thymidine kinase gene and 5′ loxP-flanked Neo cassette. The final targeting vector was linearized with PvuI for transfection.

Bruce-4 embryonic stem (ES) cells were transfected with the targeting vector by electroporation. G-418 and gancyclovir-resistant clones were screened for homologous recombination by PCR amplification as indicated. Germline chimeric mice were generated by injecting Bruce-4 ES cells into BALB/c blastocysts. Chimeric mice with a high ES cell contribution were crossed with C57BL/6 mice to generate $Hsp90aa1^{neo/+}$ mice, and the latter were crossed with CAG-Cre mice, which express cre under the control of the CMV promoter, to generate $Hsp90aa1^{-/+}$ mice. $Hsp90aa1^{-/+}$ mice were intercrossed to generate $Hsp90aa1^{-/-}$ mice. Genotyping was confirmed by genomic PCR. All mice were housed in a specific pathogen-free facility. Experiments were performed according to institutional guidelines.

The primers used to test for homologous recombination were B1 forward (within exon 3) gattggccagtttggtgttggtttttactc; B2 forward (within exon 2) tttctgaggg agctcatctccaattcatcg; B1 and B2 reverse (within the Neo cassette) tcgccttctatcgccttctt; B3 forward (within the Neo cassette) atagccgaatagcctctcca; and B3 reverse agtgctttgatactgccagtctttggttct. The primers used for genotyping of offspring were C forward (within exon 8) ttctctgaaggactactgtaccagaatgaa; and C reverse (downstream of exon 11) gtgtgggggtgcgcaaagaaaagacacatt. The primers used for evaluation of relative expression of HSP90aa1 (from exon 3 to exon 11) were D forward (within exon 3) taggctctggataaaatccgttacgagagc; and D reverse (within exon 11) gatgtgtcgtcatctccttccaggggaggc.

Surface Staining with GA–FITC. DC2.4 cells were cultured for 60 min at 37 °C in the presence of the surface HSP90 inhibitor geldanamycin (GA)–FITC, which binds to the N-terminal ATP binding site of HSP90 or control GA. After incubation, cells were washed three times and analyzed by FACS.

Antigen Presentation Assay. The cross-presentation assay for soluble or cell-associated OVA and the endogenous OVA antigen presentation assay are described in ref. 2.

Membrane Labeling and Uptake of AF647–OVA for ImageStream. To visualize and quantify the localization of pulsed OVA, the ImageStream system was used in this study using the protocol for data acquisition and analysis supplied by the manufacturer. The membranes of DCs (DC2.4 or BMDCs from WT or HSP90α-null mice, 2×10^6 cells) were labeled with PKH67 according to the protocol provided by the manufacturer, and incubated with AF647–OVA (0.5 mg/mL) for 5 min followed by washing three times. The cells were the subjected to ImageStream analysis.

Uptake of Apoptotic Cells. To confirm the uptake of apoptotic cells (cell-associated OVA donor cell) in cross-presentation (Fig. 1*E*), apoptotic cells (2.5×10^7 cells) described above were labeled with PKH26 and cocultured with PKH67-labeled BMDCs (5×10^6 cells) from WT or HSP90α-null mice for 3 h at 37 °C. Cells were washed three times and then analyzed by ImageStream.

ImageStream Data Acquisition and Analysis. PKH67-labeled DCs (2×10^6 cells) were incubated with AF647–OVA (0.5 mg/mL) for 5 min and washed three times. The cells were subjected to ImageStream analysis to determine the internalization of OVA and its translocation to the cytosol. At first, we gated events with intermediate bright field (BF) area and high aspect ratio to distinguish single cells (R1) from debris (low BF area) and cell clusters (high BF area and low aspect ratio) (Fig. S4*A*), thus limiting the analysis to intact single DCs. The aspect ratio is the minor axis divided by the major axis of each image and describes how round or oblong an object is. Out-of-focus cells with low BF contrast were excluded from the analysis. Next, double-positive cells, consisting of PKH67-labeled DCs and AF647–OVA (R2) were gated in the plots of PKH67 versus AF647 by comparison with the single color plots for each fluorophore (Fig. S4*B*). The double-positive cells included two populations: the DCs that had internalized AF647–OVA (R5 and R6) and those to which AF647–OVA was attached on the cell surface and not internalized (R4), as shown in Fig. S4*C*.

The internalization score is derived from the ratio of OVA intensity inside the cells to the total OVA intensity. The score is adjusted such that a ratio value of 0.5 (half of the OVA is inside the cell) has a score of 0, so that a ratio value less than 0.5 (more than half of the OVA is outside the cell) has a negative score (R4) and a value greater than 0.5 (more than half is inside) has a positive score (R5 and R6). The phagocytic ratio was calculated by the counts of cells with internalized OVA (R5 + R6) divided by the count of total PKH67-positive DCs (R2 + R3). To measure the relative colocalization of OVA to DC-associated organelles, we calculated the correlation between bright details of the OVA and DC image pair using the bright detail similarity (BDS) feature. Gating for colocalized events was based on visual inspection of histogram bins. Because OVA molecules are internalized and colocalized with the DC-associated organelles, the internalization score and BDS feature increases (R6). In a series of the gating procedures, the double-positive cells (R2) were divided into three populations: not internalized and not colocalized (R4), internalized and not colo-

calized (R5), and internalized and colocalized (R6) (Fig. S4*C*). Representative images of R5 and R6 are shown in Fig. S4*D*. R5 was identified as the DC population with significant proportion of internalized OVA dislocated from the endosomes to the cytosol. R6 was identified as the population in which most of the internalized OVA was still located within the endosomes.

Fluorescence Microscopy for Vesicle Counting. DCs (5×10^4 cells), DC 2.4 cells and BMDCs, grown for ~16 h on a glass-bottom dish were treated with MG115, with/without 20 μM Radicicol for 15 min. The cell membranes were stained with PKH67 on ice according to the protocol provided by the manufacturer, then pulsed with 0.5 mg/mL AF647-labeled OVA for 5 min at 37 °C and fixed. The fluorescent images of the PKH67-labeled DC (green) and AF647–OVA (red) were observed with a Keyence BZ-9000 fluorescence microscope using GFP and Cy5 filter sets, respectively. The individual images were overlaid on image processing software BZ-II analyzer and then the vesicles were counted. AF647–OVA, PKH67–DC, and their merged vesicles were defined as red, green, and yellow, respectively, by the software.

Subcellular Fractionation. BMDC or DC2.4 cells (4×10^6 cells) were treated with a proteasome inhibitor (epoxomicin: EPO or MG115) for 60 min and/or the HSP90 inhibitor radicicol for 15 min and then pulsed with 3 mg/mL OVA for 5–15 min at 37 °C. Cells were immediately transferred to 4 °C and washed four times to exclude free OVA, and subcellular fractions were separated using the ProteoExtract Subcellular Proteome Extraction kit (Calbiochem; cat. no. 539790). Fractions of each sample were subjected to Western blot (WB) analysis.

Immunoprecipitation (IP). DC2.4 cells (4×10^6 cells) were treated with 25 μM radicicol for 15 min or *Pseudomonas* exotoxin A (5 μg/mL) and/or 10 μM MG115 for 60 min at 37 °C. The cells were then incubated with biotinylated OVA (1 mg/mL) for 10 min at 37 °C in the presence of inhibitor(s). After OVA uptake, the cells were washed four times and lysed in PBS with 0.2% Nonidet P-40 and a protease inhibitor mixture. The lysate was incubated on ice for 30 min and then centrifuged for 15 min in a microfuge to pellet the insoluble debris. Mouse anti-HSP90 mAb (2A6-E9) or normal mouse IgG and then sheep antimouse IgG conjugated Dynabeads M-280 (Invitrogen) were added to the lysate and incubated at 4 °C for 2 h. Dynabeads were separated from the unbound solution with a magnet and washed three times with the lysis buffer. The precipitated samples were lysed with 4× sample buffer (4% SDS, 2-ME, 20% glycerol, and 125 mM Tris-HCl) and analyzed by SDS/PAGE and Western blotting.

Phagosome Purification. The phagosomes were purified by a modification of the method described by Dejardins (3). Latex beads (LB; 0.8 μm in a diameter, 6% solution final, Sigma) were washed three times with PBS followed by incubation with OVA (10 mg/mL) or biotinylated Japanese cedar pollen allergen Cryj1 (bCryj, 1 mg/mL) at 4 °C for electrical coupling. DC2.4 cells ($5–10 \times 10^7$) were pulsed with 200 μL of LB–OVA or LB–Cryj for 5–60 min at 37 °C. Following this step, all procedures were performed on ice. Cells were washed three times with ice-cold RPMI1640 and once with homogenization buffer (250 mM sucrose, 3 mM imidazole, pH 7.4). Pellets were resuspended in 1 mL of cold homogenization buffer and homogenized on ice using a Dounce homogenizer with a tight-fitting pestle. Cells were homogenized until about 90% of cells were broken without major breakage of the nucleus, as monitored by microscopy. Unbroken cells and nuclei were removed by centrifugation at $300 \times g$ for 5 min and supernatants were collected. Phagosomes were isolated by a sucrose step gradient ultracentrifugation method. All sucrose solutions contained 3 mM imidazole, pH 7.4. Phagosome-containing supernatants (~1 mL) were mixed with a 1.5 × volume of 62% sucrose solution and loaded on top of a 2-mL cushion of 62% sucrose. Then 2 mL of 35% sucrose, 2 mL of 25% sucrose, and 3 mL of 10% sucrose solutions were added in order, then centrifuged for 1 h at $100,000 \times g$ at 4 °C in swinging bucket rotor SW41Ti (Beckman). Phagosome-containing LB–OVA or LB–Cryj bands were collected from the interface of the 10 and 25% sucrose solutions and washed once with ICT buffer (50 mM Hepes, 78 mM KCl, 4 mM $MgCl_2$, 8.37 mM $CaCl_2$, and 10 mM EGTA, pH 7.4) for 20 min at $40,000 \times g$ in SW41Ti rotor at 4 °C. Pellets were finally resuspended in ICT buffer (100–300 μL) and used as phagosomes (LB–Ag-containing phagosome). Purified phagosomes were subjected to WB or in vitro translocation assays.

In Vitro Translocation Assay. Cytosol was obtained by the method described previously (4). DC2.4 cells or BMDCs ($2.5–5 \times 10^7$) were washed once with homogenization buffer and the pellet was resuspended in 2 mL of homogenization buffer and homogenized with Dounce-homogenizer as described above. Unbroken cells and nuclei were removed by centrifugation. The supernatant was cleared by ultracentrifugation at $12,000 \times g$ for 1 h at 4 °C in a SW55Ti rotor (Beckman) and then dialyzed overnight against ICT buffer (50 mM Hepes, 78 mM KCl, 4 mM $MgCl_2$, 8.37 mM $CaCl_2$, and 10 mM EGTA, pH 7.4) followed by measurement of cytosolic protein concentrations of BMDCs from WT and HSP90α-null mice and then adjusted to the same concentration. The purified phagosomes were incubated with ICT buffer only, cytosol, or HSP90 (volume ratio 1:9) for 30 min at 37 °C unless otherwise indicated. After incubation, the samples were separated into the pellet and supernatant by ultracentrifugation at $40,000 \times g$ for 20 min at 4 °C, and subjected to WB assays. Quantitative analysis was performed using ImageJ software.

Induction of Antigen-Specific $CD8^+$ T Cells in Vivo and ELISPOT Assay. Mice were immunized with 2×10^6 cells osmotically loaded with OVA (1 mg/mL) for cross-presentation or $OVA_{257–264}$ peptide pulsed DC2.4 i.v. One week after immunization, CD11b negative-selected $CD8^+$ T cells were purified from spleen by a magnetic bead method. ELISPOT assay for IFNγ was performed as follows: $CD8^+$ T cells ($2.5–0.6 \times 10^5$ cells) were cocultured with $OVA_{257–264}$ pulsed DC2.4 (5×10^4 cells) in medium containing 0.05 unit/mL of IL-2 in 96-well multiscreen plates (Millipore) that had been coated with anti-IFNγ. One day after the culture, cells were washed out and a biotinylated IFNγ detection Ab was added, followed by alkaline phosphatase-conjugated avidin. Spots were developed using nitro blue tetrazolium choloride/5-bromo-4-chloro-3-indolyl phosphate (NBT/BCIP) and counted using a zoom stereomicroscope. Antigen-specific spots were determined by subtraction of the numbers of spots observed in wells where $CD8^+$ T cells were cultured with epitope unpulsed DC2.4.

In Vivo Depletion of $CD8^+$ DC by Cytochrome *c*. Mice were administrated 5 mg of horse cytochrome *c* (Sigma) i.v. dissolved in PBS. Twenty-four hours after administration, splenic DCs were isolated by collagenase treatment. After Fc blocking with normal mouse IgG, the DCs were stained with antibodies to CD11c, CD4, and CD8 and then analyzed by FACSCanto II (BD).

1. Ouchida R, et al. (2008) A lysosomal protein negatively regulates surface T cell antigen receptor expression by promoting CD3ζ-chain degradation. *Immunity* 29: 33–43.
2. Ichiyanagi T, et al. (2010) Essential role of endogenous heat shock protein 90 of dendritic cells in antigen cross-presentation. *J Immunol* 185:2693–2700.
3. Desjardins M, Huber LA, Parton RG, Griffiths G (1994) Biogenesis of phagolysosomes proceeds through a sequential series of interactions with the endocytic apparatus. *J Cell Biol* 124:677–688.
4. Houde M, et al. (2003) Phagosomes are competent organelles for antigen cross-presentation. *Nature* 425:402–406.

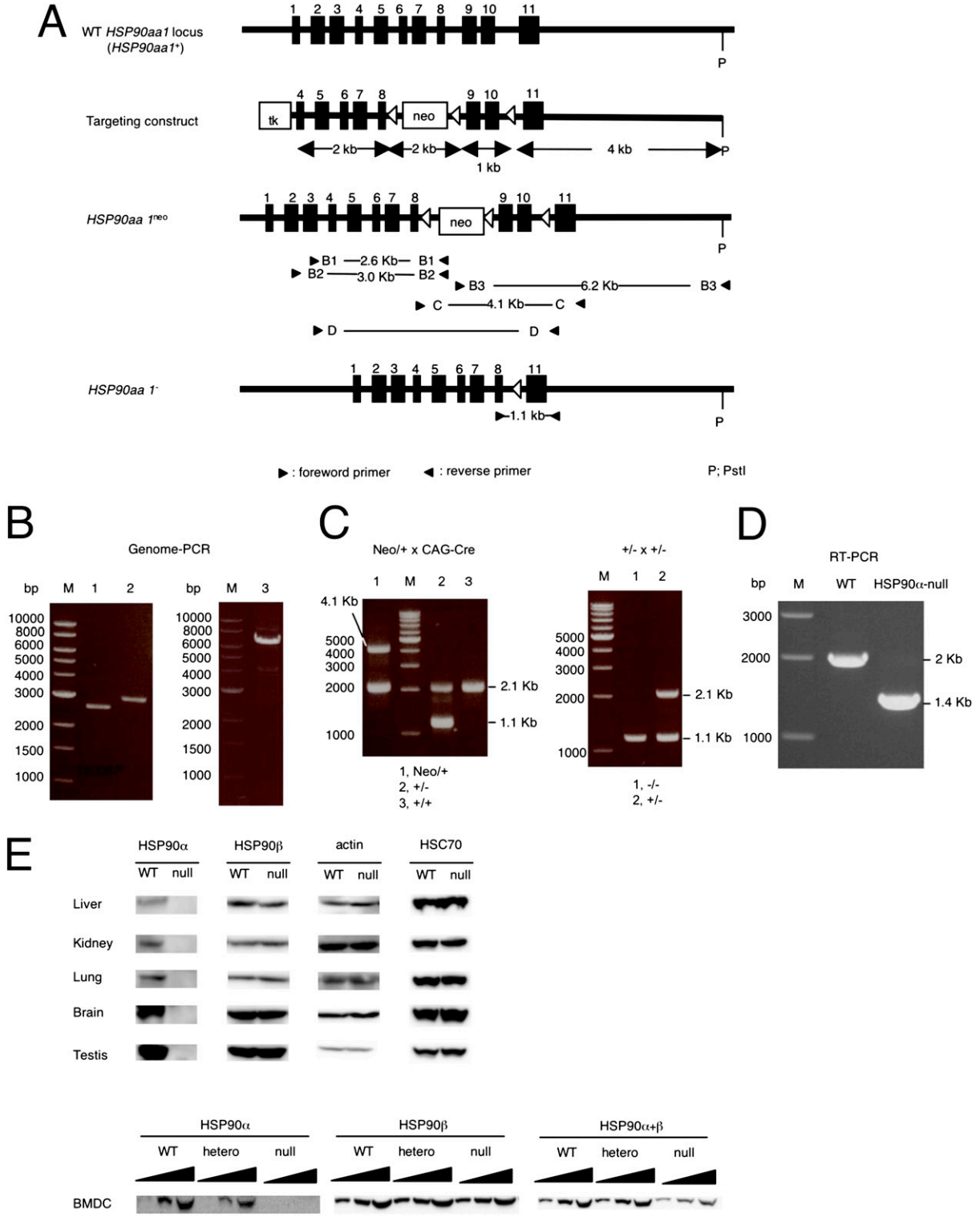

Fig. S1. Generation of HSP90α-null mice. (*A*) Schematic diagram of the mouse HSP90*aa1* genomic locus and the targeting vector used to disrupt the gene, showing the HSP90*aa1*^{neo} and HSP90*aa1*$^{-}$ mutant alleles. The primers used for genotyping of WT and mutant alleles are indicated by arrowheads. (*B*) Genomic-PCR of targeted ES cells. Primers used are depicted as B1–3 in *A*. (*C*) Results of genotyping of HSP90*aa1*$^{neo/+}$, HSP90aa1$^{+/-}$, and HSP90aa1$^{-/-}$ offspring. Primers are depicted as C in *A*. (*D*) Total RNA was purified from the liver of WT or HSP90α-null mice and converted to cDNA, followed by amplification of the region between exon 3 and exon 11. The positions of primers used are depicted as D in *A*. (*E*) Organs or BMDCs from WT or HSP90α-null mice were subjected to Western blot with the indicated antibodies.

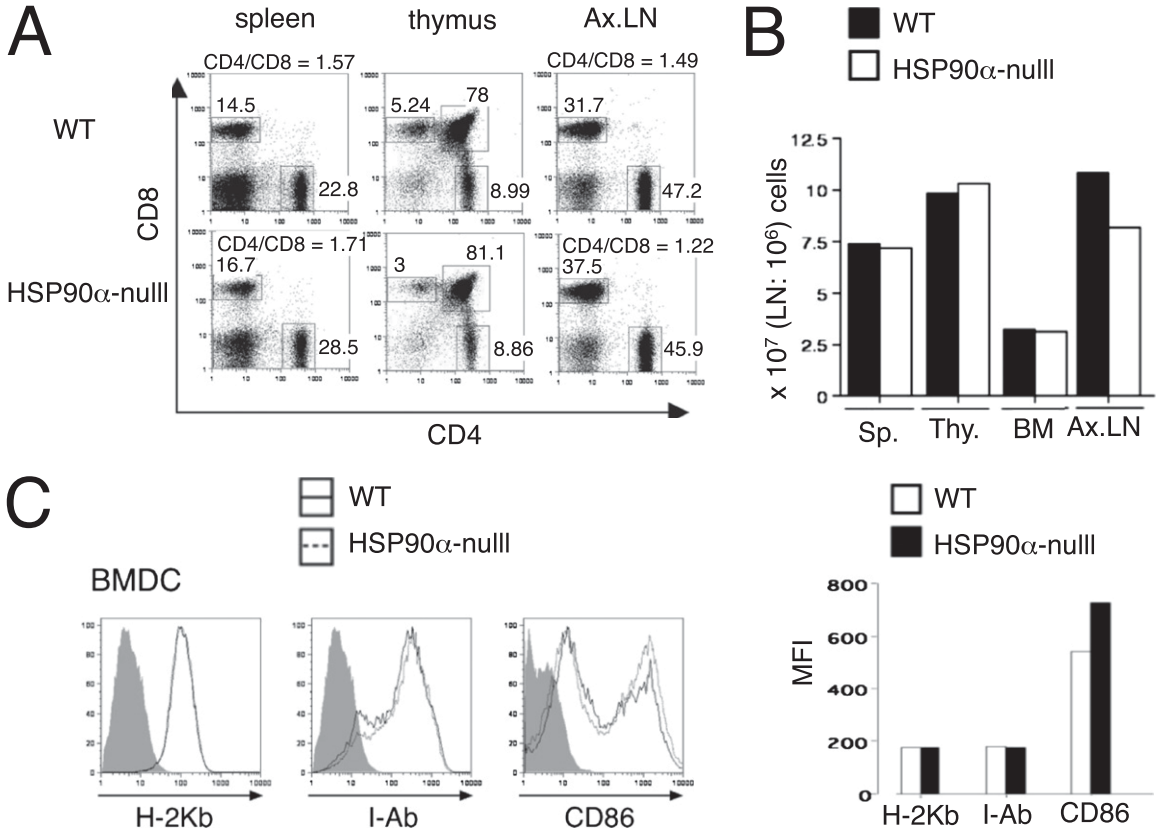

Figure S2. Phenotype of HSP90α-null mice. (*A*) Single cell suspensions were prepared from the spleen, thymus, and axillary (Ax.) LN of WT or HSP90α-null mice, then stained with fluoresceinated antibody against CD4 or CD8 and analyzed by flow cytometry. Numbers indicate the percentage of FS- and SS-gated populations. (*B*) Numbers of cells isolated from the indicated tissues. (*C*) Surface molecules expressed by BMDCs derived from WT and KO mice.

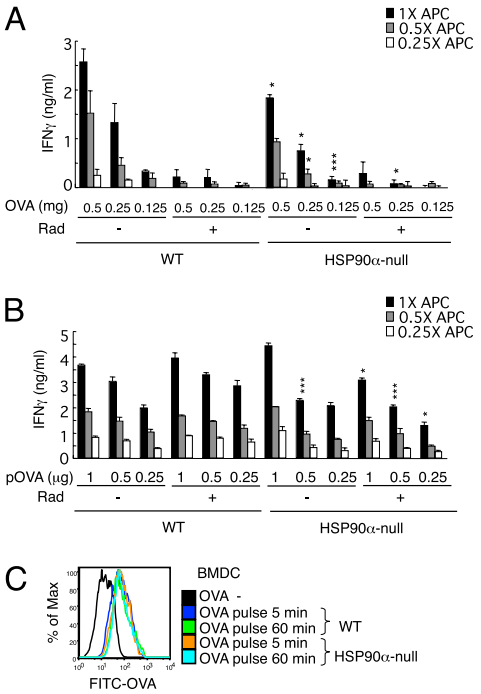

Fig. S3. Differential effects of HSP90 inhibition on Ag presentation. (*A*) BMDCs from WT and HSP90α-null mice were pulsed with OVA in culture medium with or without Rad. The procedure is similar to that described in Fig. 1*C*. (*B*) BMDCs from WT and HSP90α-null mice were transfected with pOVA and treated with or without Rad, then seeded in tissue culture wells as APC. The procedure is similar to that described in Fig. 1*D*. (*C*) BMDCs from WT and HSP90α-null mice were pulsed with FITC–OVA for 5 or 60 min at 37 °C, and then washed extensively before analysis by flow cytometry. Data are mean ± SD $*P < 0.05$; $**P < 0.01$; $***P < 0.001$. The values were compared between WT and HSP90α-null.

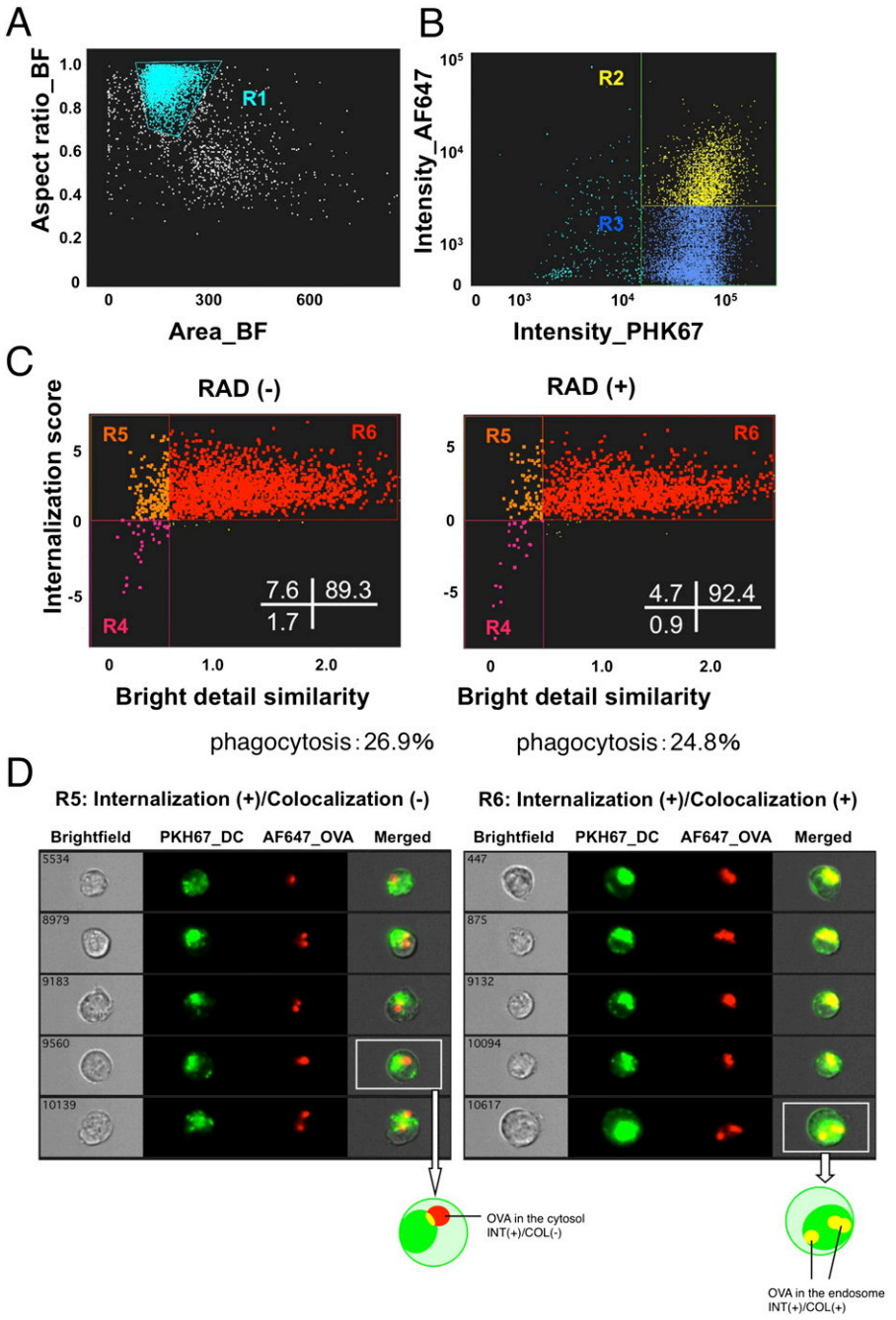

Fig. S4. The principle of ImageStream and prevention of Ag translocation by the HSP90 inhibitor RAD. PKH67-labeled DC2.4 cells (5×10^6) were incubated with AF647–OVA (1 mg/mL) for 5 min and washed three times. The cells were subjected to ImageStream analysis to determine internalization of OVA and its intracellular location. The ImageStream imaging cytometer can acquire up to six different spatially registered images (bright field, dark field, and four fluorescent) per cell at very high rates using a digital CCD camera. At least 10,000 images were collected for each sample. (*A*) Aspect ratio (the minor axis divided by the major axis of each image) bright field (BF) by area BF profiles of events in BMDCs. Single cells (R1) were gated from debris (low BF area) and cell clusters (high BF area and low aspect ratio). (*B*) Two-color plot. DC2.4 cell membranes labeled by PKH67 do (R2) or do not (R3) take up AF647–OVA. (*C*) Populations of PKH67 and AF647 double-positive cells were replotted for bright detail similarity (*x*-axis) versus internalization score (*y*-axis) to determine the localization of AF647–OVA, OVA attached to the surface (R4), OVA in the endosome (R6), and OVA in the cytosol (R5). The internalization score represents the ratio of AF647–OVA intensity inside the cells to the total AF647–OVA intensity. The score is adjusted such that a ratio value of 0.5 (half of the OVA is inside the cell) has a score of 0. Thus, a ratio value less than 0.5 (more than half of the OVA is outside the cell) has a negative score (R4), whereas a value greater than 0.5 (more than half is inside) has a positive score (R5 and R6). The phagocytic ratio was calculated by the counts of cells with internalized OVA (R5 + R6) divided by the count of PKH67-positive DC2.4 cells (R2 + R3). To measure the relative colocalization of OVA to DC-associated organelles derived from the surface membrane, we calculated the correlation between bright details of the OVA and DC image pair using the bright detail similarity (BDS) feature. The BDS feature correlates with only the portion of each image in the optimal plane of focus and ignores data related to background pixels within the cells. Gating for co-localized events was judged on the basis of visual inspection of the histogram bins. Because the OVA molecules are internalized and colocalized to the DC-associated organelles, the internalization score and BDS feature increases (R6). In a series of the gating procedures, double-positive cells (R2) were divided into three populations: not internalized and not colocalized (R4, OVA attached to the surface), internalized and not colocalized (R5, OVA translocated to the cytosol), and internalized and colocalized (R6, OVA in the endosome). (*D*) Representative images from at least 10,000 images collected for this analysis.

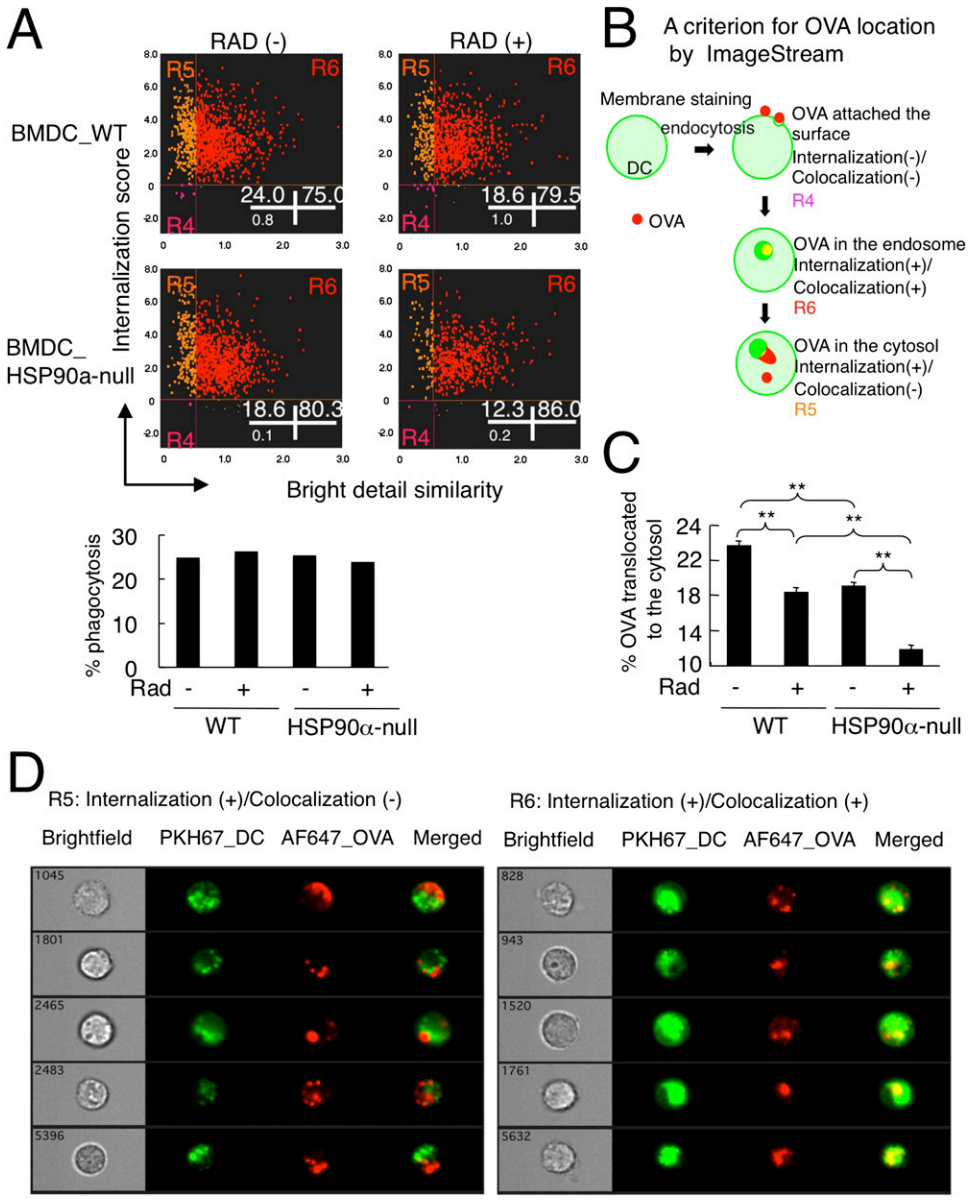

Fig. S5. Quantitative analysis of the cellular localization of pulsed OVA using ImageStream. BMDCs from WT or HSP90α-null mice were treated with MG115, with/without Rad for 15 min. The cells were stained with PKH67 on ice for visualization of the membranes, then pulsed with AF647-labeled OVA for 5 min at 37 °C and fixed. Samples were analyzed by ImageStream. (*A*) Internalization score by bright detail similarity profiles of events in BMDCs as described in *Materials and Methods*. The percentage of phagocytosis in WT RAD (–), WT RAD (+), HSP90α-null RAD (–), and HSP90α-null RAD (+) was 24.9, 26.3, 25.4, and 23.9%, respectively. (*B*) Criteria used to define location of OVA. (*C*) The percentage of OVA translocated to the cytosol, calculated as described in *Materials and Methods* and Fig. S4. Data are mean ± SD of two separate experiments. $^{**}P < 0.01$. (*D*) Representative images from at least 10,000 images collected for this analysis.

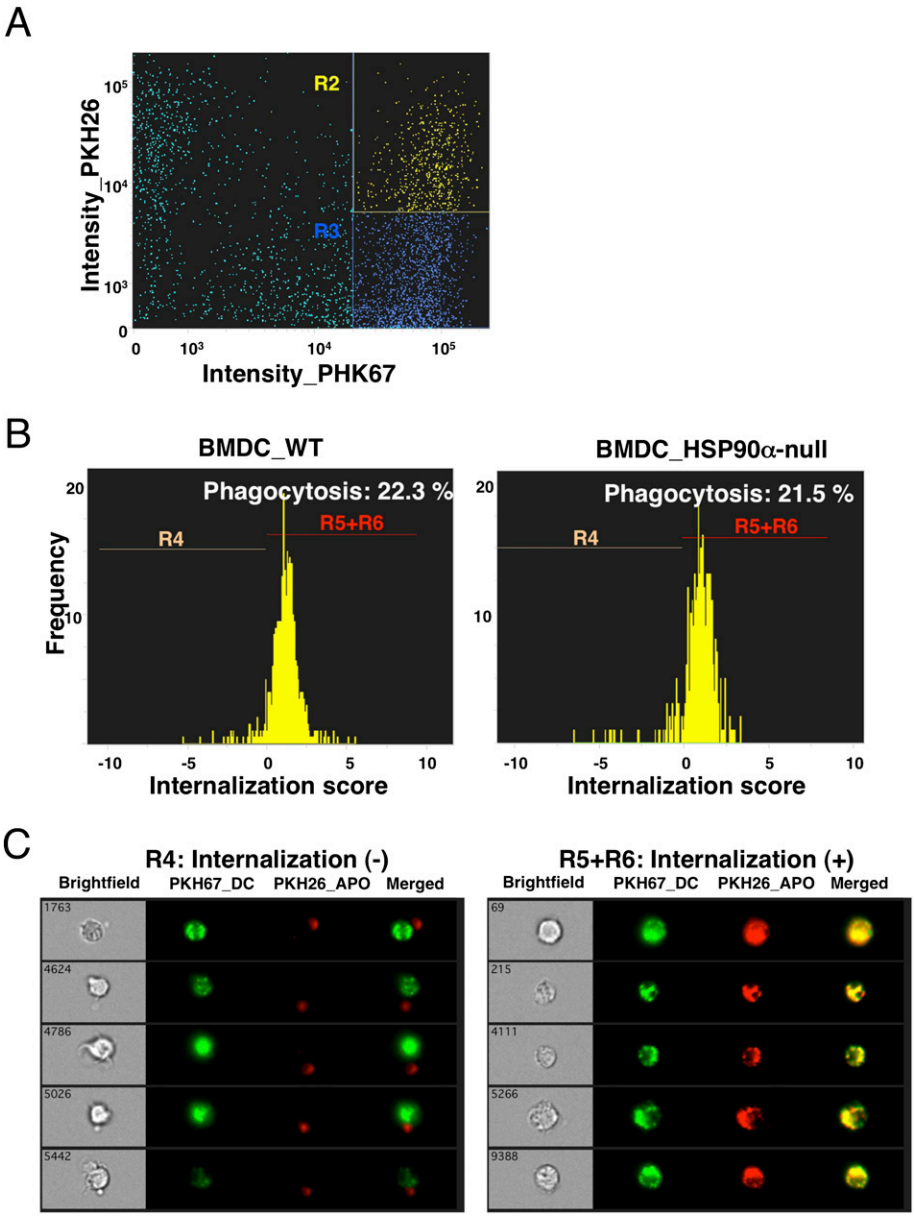

Fig. S6. Phagocytosis by BMDCs from HSP90α-null mice is comparable to that from WT mice. The cell membranes of UV-irradiated apoptotic cells from TAP1 KO cells (APO) were labeled with PKH26. BMDCs were labeled with PKH67 and cocultured with PKH26 labeled APO for 3 h, then analyzed by ImageStream. (*A*) Two-color plot. (*B*) Double-positive cells were gated and then analyzed. Histogram of internalization score: <0 represents APO attached to the surface of DC (R4); >0 represents APO internalized by DC (R5 and R6). Percentage of phagocytosis is shown. (*C*) Representative pictures from at least 10,000 images.

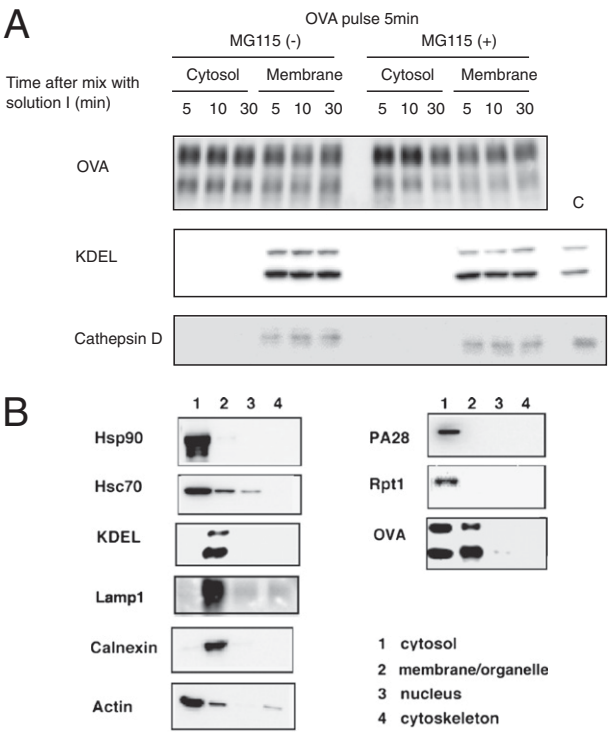

Fig. S7. Evaluation of the efficiency of subcellular fractionation. DC2.4 cells treated with/without the proteasome inhibitor MG115 were pulsed with 3 mg/mL of OVA for 5 min. After extensive washing, the cells were fractionated using a subcellular fractionation kit (Calbiochem). (*A*) Leakage of luminal proteins from the membrane/organelle fraction to the cytosol fraction was evaluated. Solution I (cytosol extraction buffer) was mixed with the cell pellet for the indicated time and then subjected to extraction of the membrane/organelle fraction. (*B*) Fractions were analyzed by Western blot with the indicated antibodies.

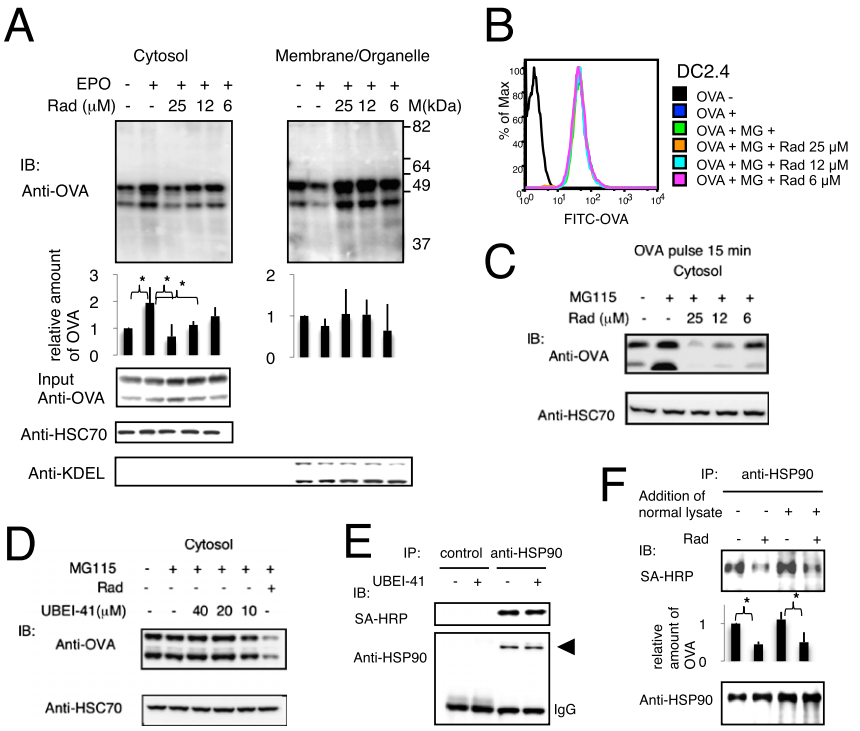

Fig. S8. (*A*) DC2.4 cells were treated with Rad and/or the proteasome inhibitor epoxomicin (EPO; 10 μM) and pulsed with 3 mg/mL of OVA for 5 min. After washing six times, cells were fractionated. Cytosol and membrane/organelle fractions were subjected to Western blot, using the indicated antibodies. (*B*) DC2.4 cells were treated with Rad and/or proteasome inhibitor MG115 (10 μM) and pulsed with 0.4 mg/mL of FITC–OVA for 5 min. After extensive washing, the internalization efficiency was monitored by FACS analysis. (*C*) As in *A*, DC2.4 cells were treated with Rad and/or MG115 (10 μM) and pulsed with 3 mg/mL of OVA for 15 min. Cytosol and membrane/organelle fractions were subjected to Western blot using the indicated antibodies. (*D*) DC2.4 cells were treated with UBE1-41 and/or MG115, Rad, and pulsed with 3 mg/mL of OVA for 15 min and then subjected to subcellular fractionation. (*E*) DC2.4 cells treated with UBE1-41 were pulsed with biotin–OVA for 15 min. The cell lysates were used for immunoprecipitation with anti-HSP90 mAb or control IgG. OVA was detected with streptavidin (SA)–HRP. Arrowhead indicates HSP90. (*F*) Examination of possible postlysis association of HSP90 with OVA. DC2.4 cells treated with/without Rad were pulsed with biotin–OVA and lysed. The lysates were added with/without normal lysate from Rad-untreated DC2.4 cells and IP was performed with anti-HSP90. Biotin–OVA was detected by SA–HRP. Note that addition of normal lysate had no influence on the pattern of coprecipitated OVA. One representative experiment of at least three is displayed.

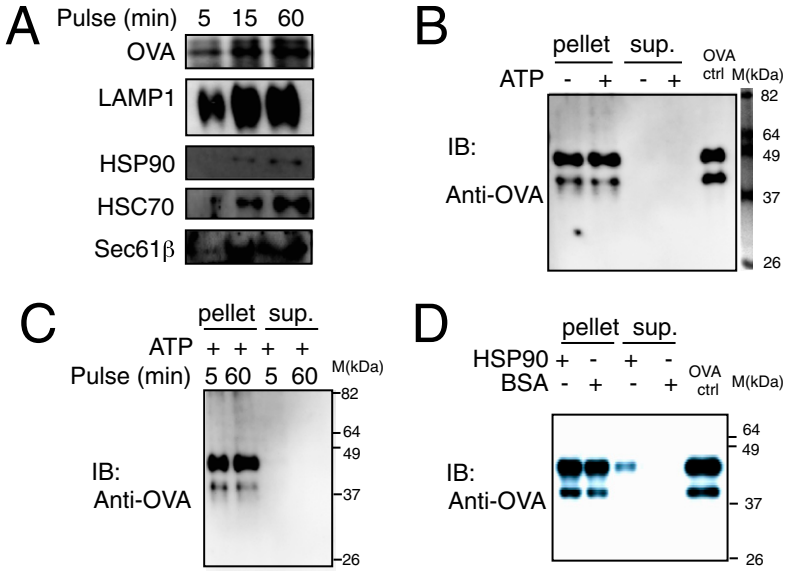

Fig. S9. (*A*) DC2.4 cells (5×10^7) were pulsed with OVA–LB for 5, 15, and 60 min, and the phagosomes were purified. The proteins associated with the phagosomes were detected by Western blot using the indicated antibodies. (*B*) Phagosomes from DC2.4 cells pulsed with OVA–LB for 5 min were incubated with/without ATP for 30 min at 37 °C. After centrifugation, the pellets and the supernatants were blotted with anti-OVA Ab. (*C*) DC2.4 cells were incubated with OVA–LB for 5 min or 60 min, after which the phagosomes were purified and incubated for 30 min at 37 °C in the presence of ATP. After centrifugation, the pellets and the supernatants were blotted with anti-OVA Ab. (*D*) Phagosomes containing OVA–LB was used for the Ag-translocation assay in the presence of either HSP90 purified from Meth A (5 μg) or BSA (10 μg).